

## ON CERTAIN ASPECTS OF GLOBAL AND LOCAL BUCKLING MODES IN THIN-WALLED COLUMN-BEAMS

ZBIGNIEW KOŁAKOWSKI

*Department of Strength Materials and Structures (K12)*

*Technical University of Łódź*

In the design of thin-walled column-beams must be taken into account the overall instability and the instability of component plates in the form of local plate buckling. This investigation is concerned with thin-walled closed and open cross-section elastic beams under axial compression or a constant bending moment. Buckling analysis includes cross-section distortion. The beams are assumed to be simply supported at the ends. The asymptotic expansion established by Byskov and Hutchinson is employed in the numerical calculations in the form of the transition matrix method. The calculations have been done for several types of beams.

### Notation

$a_{ijJ}$	-	postbuckling coefficients in the nonlinear equilibrium equations (2.8) (Byskov and Hutchinson, 1977)
$b_i$	-	width of the $i$ th wall of beam
$D_i$	-	plate rigidity of the $i$ th wall
$E$	-	Young modulus
$h_i$	-	thickness of the $i$ th wall of the beam
$l$	-	length of the beam
$m$	-	number of axial half-waves of the $n$ th mode
$M_{ix}, M_{iy}, M_{ixy}$	-	bending moment resultants for the $i$ th wall
$n$	-	number of mode
$N$	-	number of interacting modes
$N_{ix}, N_{iy}, N_{ixy}$	-	in-plane stress resultants for the $i$ th wall

$N_{ix}^{(n)}, N_{iy}^{(n)}, N_{ixy}^{(n)}$	– in-plane stress resultants for the $i$ th wall in the first order approximation
$Q_{iy}^*$	– Eq (2.5)
$u_i, v_i, w_i$	– displacement components of the $i$ th wall middle surface
$u_i^0, v_i^0, w_i^0$	– pre-buckling displacement fields
$u_i^{(n)}, v_i^{(n)}, w_i^{(n)}$	– buckling displacement fields
$\Delta$	– load factor
$\lambda$	– scalar load parameter
$\lambda_n$	– value of $\lambda$ at the bifurcation mode number $n$
$\xi_n$	– amplitude buckling mode number $n$
$\bar{\xi}_n$	– imperfection amplitude corresponding to $\xi_n$
$\sigma_n^* = \sigma_n 10^3 / E$	– dimensionless stress of the mode number $n$ .

## 1. Introduction

Analysis of buckling in conservative systems belongs to the main problems that have been studied in mechanical sciences for a number of years. One of the most important trends in the investigation of the stability of thin-walled structures has been the problem of the interaction of various buckling modes (the so-called coupled buckling).

Analysis of the results obtained by the author in interactive buckling investigation together with some published reports have drawn the attention again to the questions of global and local loss of stability in thin-walled structures.

Thin-walled structures consisting of plate elements having a number of buckling modes differing from one another both in quantitative (e.g. by the number of half-waves) and in qualitative (e.g. by global and local buckling) respects. Due to the orthogonality of linear buckling modes the critical load values are determined independently for different modes. In the case of finite displacements different buckling modes are interrelated even under loads close to their critical values (eigenvalues of a respective boundary problem). The investigation of stability of equilibrium states requires an application of a non-linear theory that enables one to estimate the influence of different factors on the structure behaviour (for instance, how geometrical changes affect the distribution of internal and external force).

The linear theory which allowed one to separate the two different buckling

modes has had a strong influence on the understanding of the non-linear theory of stability. The allowance for interactive buckling is necessary for the determination of limiting load capacity and of the imperfection sensitivity of structures close to optimum where the values of critical loads are identical or nearly so. In the case when the post-buckling behaviour of each mode taken separately is stable, their interaction may result in an unstable behaviour, and, consequently, in greater imperfection sensitivity.

The concept of interactive buckling involves the general asymptotic theory of stability. Of all versions of the general non-linear theory, the Koiter theory (cf Koiter, 1976) of conservative systems is the most popular owing to its general character and development, even more so after Byskov and Hutchinson (1977) formulated it in a convenient fashion. In this theory the perturbation method is used for the analysis of equilibrium states. The expression for potential energy of the system expands in a series relative to the amplitudes of linear modes near the point of bifurcation; the latter generally corresponds to the minimum value of critical load (the so-called bifurcation load). Therefore a precise determination of eigenvalues and eigenmodes for different buckling modes is an important factor enabling a more detailed analysis of the structure's behaviour.

A rapid development of science and technology as well as a widespread use of computer aided methods (CAD/CAM) enables a more and more perfect structure designing; in accordance with the theory of catastrophes, these structures show singularities of increasing order. The safety and reliability requirements of thin-walled structures are also more and more rigorous and can be matched only if investigations are carried out continuously.

Mathematical models tend to a higher precision and closer approximation of real structures which enables us to analyse more and more exactly the phenomena occurring during and after the loss of stability.

A more comprehensive review of literature concerning interactive buckling have been done by Ali and Sridharan (1988), Manevich (1981), (1982), (1985) and (1988), Moellmann and Goltermann (1989), Pignataro and Luongo (1987), Sridharan and Ali (1985) and (1986), Sridharan and Peng (1989) and Kolakowski (1987b) and (1989b).

In the present paper the buckling analysis of thin-walled structures under nonuniform compression in the elastic range is examined on the basis of the Byskov and Hutchinson method with the co-operation between all the walls of the structures being taken into account. The study is based on the numerical method of transition matrix. The background of this method has been discussed by Unger (1969), Klöppel and Bilstein (1971) and Bilstein (1974). An attractive feature of this method is that it is capable of describing the

complete range of behaviour of the thin-walled structures from global to local stability. In the solution obtained, the effects of interaction of certain modes having the same wavelength, the shear lag phenomenon and also the effect of cross-sectional distortions are included.

## 2. Structural problem

The long thin-walled prismatic beams of length  $l$  and composed of plane, rectangular plate segments interconnected along longitudinal edges, simply supported at both ends are considered.

A cross-section of this structure consisting of a few plates and assumed local Cartesian coordinate systems are presented in Fig.1.

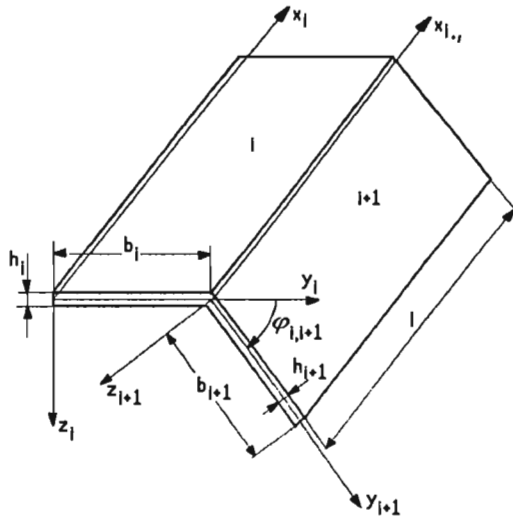


Fig. 1. Prismatic plate structure and the local coordinate system

The membrane strains of the  $i$ th wall are as follows

$$\begin{aligned}\varepsilon_{ix} &= u_{i,x} + \frac{1}{2}(w_{i,x}^2 + v_{i,x}^2) \\ \varepsilon_{iy} &= v_{i,y} + \frac{1}{2}(w_{i,y}^2 + u_{i,y}^2) \\ 2\varepsilon_{ixy} &= \gamma_{ixy} = u_{i,y} + v_{i,x} + w_{i,x}w_{i,y}\end{aligned}\quad (2.1)$$

while the bending strains are given by

$$\kappa_{ix} = -w_{i,xx} \qquad \kappa_{iy} = -w_{i,yy} \qquad \kappa_{ixy} = -w_{i,xy} \qquad (2.2)$$

The differential equilibrium equations resulting from the virtual work principle for single wall can be written as

$$\begin{aligned} -N_{ix,x} - N_{ixy,y} - (N_{iy}u_{i,y})_{,y} &= 0 \\ -N_{iy,y} - N_{ixy,x} - (N_{ix}v_{i,x})_{,x} &= 0 \\ D_i \nabla \nabla w_i - (N_{ix}w_{i,x})_{,x} - (N_{iy}w_{i,y})_{,y} - (N_{ixy}w_{i,x})_{,y} - (N_{ixy}w_{i,y})_{,x} &= 0 \end{aligned} \qquad (2.3)$$

The geometrical and statical continuity conditions at the junctions of plates may be written in the form

$$\begin{aligned} u_{i+1} \Big|_0^+ &= u_i \Big|^+ \\ w_{i+1} \Big|_0^+ &= w_i \Big|^+ \cos \varphi - v_i \Big|^+ \sin \varphi \\ v_{i+1} \Big|_0^+ &= w_i \Big|^+ \sin \varphi + v_i \Big|^+ \cos \varphi \\ w_{i+1,y} \Big|_0^+ &= w_{i,y} \Big|^+ \\ D_{i+1}(w_{i+1,yy} + \nu w_{i+1,xx}) \Big|_0^+ - D_i(w_{i,yy} + \nu w_{i,xx}) \Big|^+ &= 0 \\ N_{(i+1)y} \Big|_0^+ - N_{iy} \Big|^+ \cos \varphi - Q_{iy}^* \sin \varphi &= 0 \\ Q_{(i+1)y}^* \Big|_0^+ + N_{iy} \Big|^+ \sin \varphi - Q_{iy}^* \Big|^+ \cos \varphi &= 0 \\ N_{(i+1)xy} \Big|_0^+ - N_{ixy} \Big|^+ &= 0 \end{aligned} \qquad (2.4)$$

where:  $Q_{iy}^*$  is an equivalent the Kirchhoff transverse force

$$Q_{iy}^* = N_{iy}w_{i,y} + N_{ixy}w_{i,x} - D_i[w_{i,yyy} + (2 - \nu)w_{i,xy}] \qquad (2.5)$$

$$\varphi \equiv \varphi_{i,i+1}$$

The prebuckling solution consists of homogeneous fields which are assumed as

$$u_i^0 = -x_i \Delta \qquad v_i^0 = \nu y_i \Delta \qquad w_i^0 = 0 \qquad (2.6)$$

where  $\Delta$  is a linear function of  $y$  according to the actual loading. This loading is specified as the product of a unit loading system and a scalar load factor  $\Delta$ .

The boundary conditions permit the first order solution to be written

$$\begin{aligned} u_i^{(n)} &= U_i^{(n)}(y) \cos \frac{m\pi x}{l} \\ v_i^{(n)} &= V_i^{(n)}(y) \sin \frac{m\pi x}{l} \\ w_i^{(n)} &= W_i^{(n)}(y) \sin \frac{m\pi x}{l} \end{aligned} \quad (2.7)$$

where:  $U_i^{(n)}(y)$ ,  $V_i^{(n)}(y)$ ,  $W_i^{(n)}(y)$  (with the  $m$ th harmonic) are initially unknown functions using the modified method of transition matrix. The restraint conditions on the unloaded longitudinal edges of the adjacent plates are determined by applying the variational principle. The system of differential equilibrium equations (2.3) is solved by the modified reduction method in which the state vector of the final edge is derived from the state vector of the initial edge by numerical integration of the differential equations in the  $y$ -direction using the Runge-Kutta formulae.

The global buckling mode occurs at  $m = 1$  and the local modes at  $m > 1$  (with  $b_i \ll l$ ). Each buckling mode is normalized so that the maximum normal displacement is equal to the thickness of the first constituent plate.

The equations of equilibrium take the form

$$\left(1 - \frac{\lambda}{\lambda_J}\right) \xi_J + a_{ijJ} \xi_i \xi_J + \dots = \frac{\lambda}{\lambda_J} \bar{\xi}_J \quad J = 1, 2, \dots, N \quad (2.8)$$

Formulae for the postbuckling coefficients  $a_{ijJ}$  involve only the buckling modes.

### 3. Results

Many varieties of typical structures were tested and taking into account the above in all cases good or even very good agreement was found with the results known from the literature (wide stiffened plate, open- and closed-section column-beams).

From the calculations carried out basic varieties were selected of typical thin-walled column-beams with open and closed cross-sections.

3.1. Closed column

For a compressive thin-walled column of square cross-section the geometrical dimensions of which are the following (cf Kolakowski, 1989b)

$$\frac{l}{b_i} = 67.39 \qquad \frac{b_i}{h_i} = 100.0 \qquad \nu = 0.3$$

Fig.2a presents the global buckling modes and Fig.2c a few first local buckling modes at  $m = 67$ . Fig.2b shows only the displacements  $v$  for the top and bottom flanges, and the displacement  $w$  for the web. These displacements correspond to global buckling modes for the column in the scale of 10000:1.

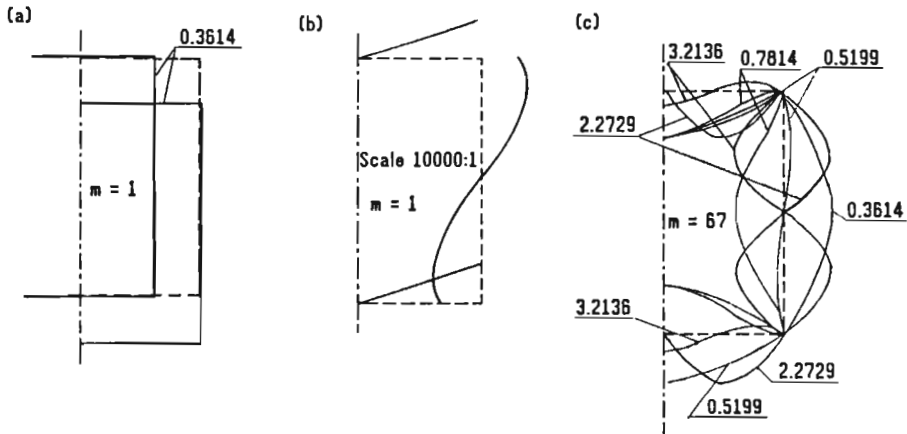


Fig. 2. Several global and local modes for square box-column

It can be concluded from comparison of the obtained stress values  $\sigma_1^* = 0.3614$ , corresponding to the global buckling, with the stress values  $\sigma_E^* = 0.3621$ , calculated from the Euler's formula, that taking into account the additional expressions  $0.5v_{i,x}^2$  and  $0.5u_{i,x}^2$  in formulae for  $\epsilon_{ix}$  and  $\epsilon_{iy}$ , respectively, has provided a true description of the global and local buckling of thin-walled structures.

Fig.3 ÷ Fig.5 present plot of in-plane stress resultants  $N_{ix}^{(n)}$ ,  $N_{iy}^{(n)}$ ,  $N_{ixy}^{(n)}$  distributions for the global and local buckling modes. On the basis of the plots presented regarding the global mode (in Fig.3 ÷ Fig.5) we find that  $N_{ix}^{(1)}$  is the only component that can be taken with accuracy sufficient for practical purposes, while in the local mode the force components  $N_{ix}^{(2)}$ ,  $N_{iy}^{(2)}$ ,  $N_{ixy}^{(2)}$  are of the same order and attain their maximum values at (or near) the corner.

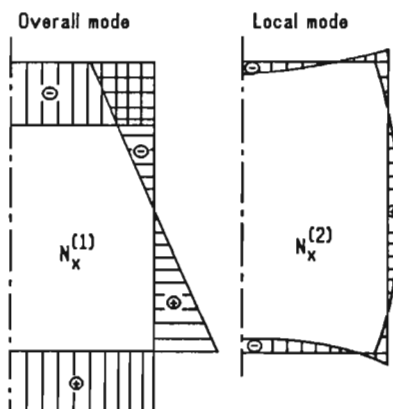


Fig. 3. Plot of in-plane stress resultant  $N_x^{(1)}$  for global and local buckling modes

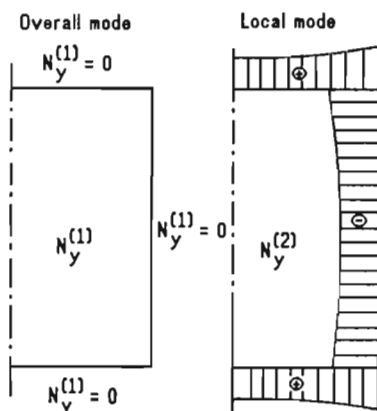


Fig. 4. Plot of in-plane stress resultant  $N_y^{(1)}$  for global and local buckling modes

Furthermore, assuming simplified boundary conditions for the walls at the corners, it is not always possible to neglect the equivalent shearing Kirchhoff forces  $Q_{iy}^*$ , the values of these being respectively  $Q_{(i-1)y}^{*(2)} = N_{iy}^{(2)}$  and  $Q_{iy}^{*(2)} = N_{(i-1)y}^{(2)}$ .

The constructions designed in the forms of a wide plate and a closed cylindrical shell, respectively, reinforced by longitudinal stiffeners have been analysed in a most detailed manner with the application of general methods of stability analysis of structures.

Since the effect of shear lag is more pronounced in stiffened plates than in unstiffened plates of the same extensional rigidity, the designer is even more



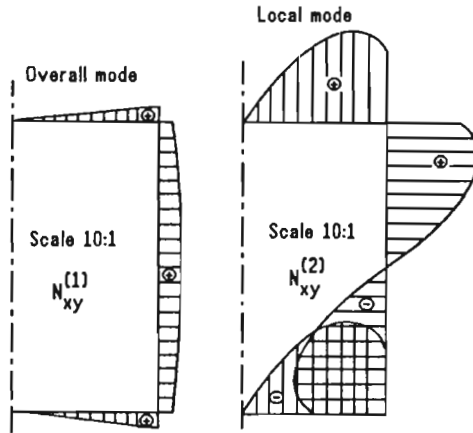


Fig. 5. Plot of in-plane stress resultant  $N_{xy}^{(1)}$  for global and local buckling modes

concerned with the interaction of shear lag and collapse by buckling in the case of wide stiffened flanges. As regards the skin plate (cf Kolakowski, 1989a), the shear lag effect on a distribution of  $N_{ix}^{(1)}$  stress can be observed. In this case the sectional force components  $N_{ix}^{(1)}$ ,  $N_{iy}^{(1)}$ ,  $N_{ixy}^{(1)}$  are of the same order.

Omission of the in-plane stress resultants  $N_{ix}^{(n)}$ ,  $N_{iy}^{(n)}$ ,  $N_{ixy}^{(n)}$  in the analysis may lead to quite large differences as compared with the case when they are taken into account (for more detailed analysis see Kolakowski (1987b) and (1993)). The technical theory of stiffened plates even if used for stiffened plates may lead to considerable discrepancies in comparison with the assumed description of global buckling by means of the nonlinear von Karman's equations (cf Kolakowski, 1987b and 1989a).

In the buckling analysis of the thin-walled stiffened plate the local mode of skin plate and the local mode of stiffeners should be taken into account (cf Kolakowski, 1987b, 1988 and 1989a; Manevich, 1981, 1982, 1985 and 1988).

### 3.2. Open beams

The buckling analysis of thin-walled open beams has been investigated in cold formed steel structures.

Fig.6 shows the cross-section of the considered beams. Let us consider the channel-section beam analysed by Benito and Sridharan (1984-85) shown, in

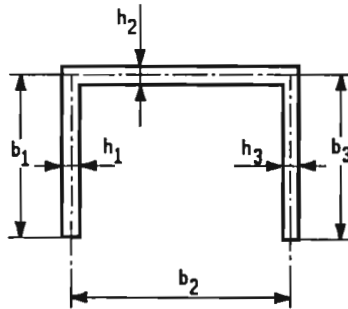


Fig. 6. Open cross-section considered

Fig.6, dimensions of which are

$$\begin{array}{llll} \frac{b_1}{b_2} = 0.5 & \frac{b_3}{b_2} = 0.5 & \frac{h_1}{h_2} = 1 & \frac{h_3}{h_2} = 1 \\ \frac{b_2}{h_2} = 50 & \frac{l}{b_2} = 13 & \nu = 0.3 & \end{array}$$

The ratio of the flexural-torsional (primary global) stress to the primary local stress is found here as equal to 0.99 and the ratio of purely flexural (secondary global) stress to the local stress is determined as equal to 1.42 (Benito and Sridharan (1984-85) give the values of 1.04 and 1.44, respectively).

Fig.7 presents the two first global and local values of nondimension stresses  $\sigma_n^*$  in terms of the angle  $\varphi_{i,i+1}$  between walls. In this figure an auxiliary angle  $\alpha$  is introduced between walls of the channel ( $\varphi_{i,i+1} = 90^\circ \pm \alpha$ ). If  $\alpha$  changes, a substantial decrease is found in the value of the first overall load  $\sigma_1^*$  at angles  $\varphi_{12} = 90^\circ + \alpha$ ;  $\varphi_{23} = 90^\circ - \alpha$ ; the second global load  $\sigma_3^*$  ( $m = 1$ ) at angles  $\varphi_{12} = \varphi_{23} = 90^\circ + \alpha$ ; and a relatively small change in the value of  $\sigma_3^*$  at  $\varphi_{12} = 90^\circ + \alpha$  and  $\varphi_{23} = 90^\circ - \alpha$ . In the latter case the stress  $\sigma_3^*$  reaches its maximum value at  $\alpha = \pm 10^\circ$ . The exception is the first overall load  $\sigma_1^*$  at  $\varphi_{12} = \varphi_{23} = 90^\circ + \alpha$  which increases along with the increase in angle  $\alpha$ . It is a result of different buckling modes for different  $\alpha$  angles (see Fig.8).

At the same time the values of local load  $\sigma_2^*$  ( $m = 10$ ) remain virtually constant, their changes being practically negligible. This fact can be explained in the following way. While determining approximate values of load, corresponding to the local modes under conditions of meeting, we are able to take into account only the situation where the angle is constant and bending moments are equal, moreover, the deflection function  $w_i$  for individual plates

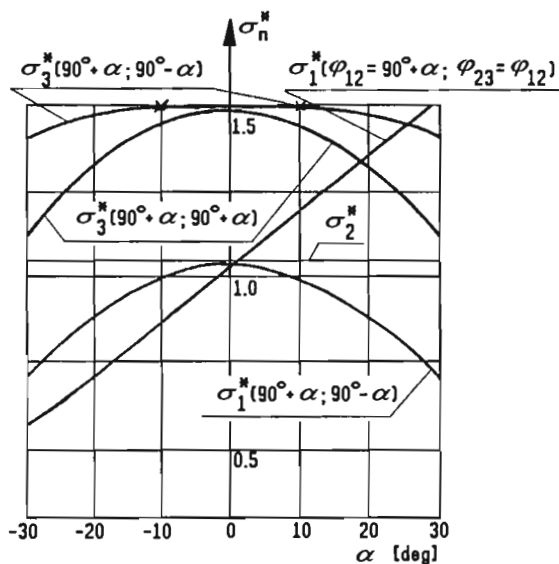


Fig. 7. Relationship between stresses  $\sigma_n^*$  and the auxiliary angle  $\alpha$

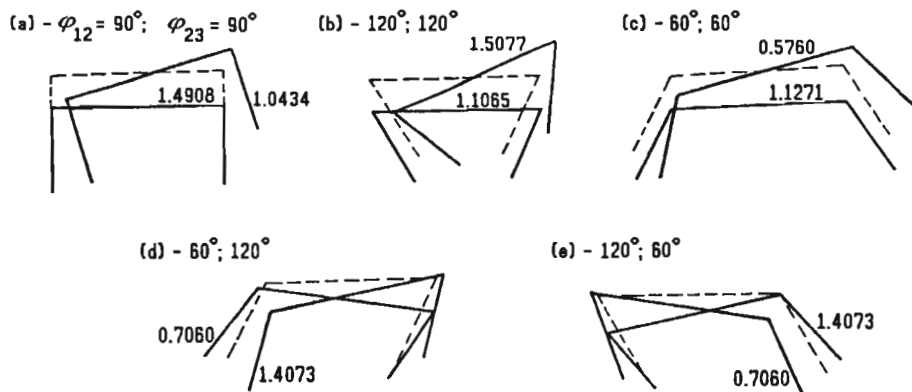


Fig. 8. Two global modes at different angles  $\varphi_{i,i+1}$

is assumed to be zero at the points of the junction.

The Byskov and Hutchinson theory, applied here, reduces all kinds of imperfections to the ones which correspond to initial deflections of a thin-walled structure: non-linear coefficients  $a_{ijJ}$  in Eq (2.8) remain constant. Not all kinds of imperfections can be reduced to a single type. Calculations of slight deviations of load and geometrical dimensions allow us to obtain "proper" imperfection sensitivity of constructions as well as to find out, whether the assumed model of a single type imperfection is correct.

Fig.8a ÷ Fig.8e present the first two global buckling modes for various extreme values of angles between walls of the channel under consideration (Fig.7). In the cross-section with a vertical symmetry axis (Fig.8a,b,c) two distinct global modes can be found, namely the flexural-torsional and the flexural (Euler) ones. In the two other cases (Fig.8d,e) this distinction is more difficult to find.

In the thin-walled column analysed by Benito and Sridharan (1984-85), their dimensions being as follows

$$\begin{array}{llll} \frac{b_1}{b_2} = 0.5 & \frac{b_3}{b_2} = 0.5 & \frac{h_1}{h_2} = 1 & \frac{h_3}{h_2} = 1 \\ \frac{b_2}{h_2} = 50 & \frac{l}{b_2} = 7.8 & \nu = 0.3 & \end{array}$$

the ratio of the global stress value corresponding to the flexural-torsional buckling (the primary global mode) to the stress value of the local mode is 2.385, while the ratio of the stress of the global Euler mode (the secondary global mode) to the stress of the local mode is 3.545 (Benito and Sridharan (1984-85) give the values of 2.63 and 4.22, respectively). Thus taking into account the components:  $u_n^{(i)} \neq 0$ ,  $v_n^{(i)} \neq 0$ ,  $w_n^{(i)} \neq 0$  in the first order displacement field causes a decrease in the global stress values.

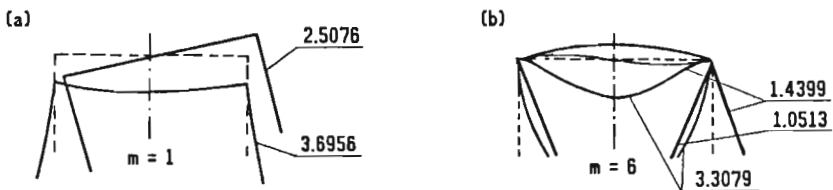


Fig. 9. Global and local buckling modes

Fig.9a shows the two global buckling modes for the considered channel. In this case two kinds of buckling can be seen: flexural-torsional and flexural.

It should be noted that the obtained stress values corresponding to global buckling modes are less perceptible than the stress values calculated for the bar model (Benito and Sridharan, 1984-85). In the other case Fig.9(b) presents a few local modes at  $m = 6$ .

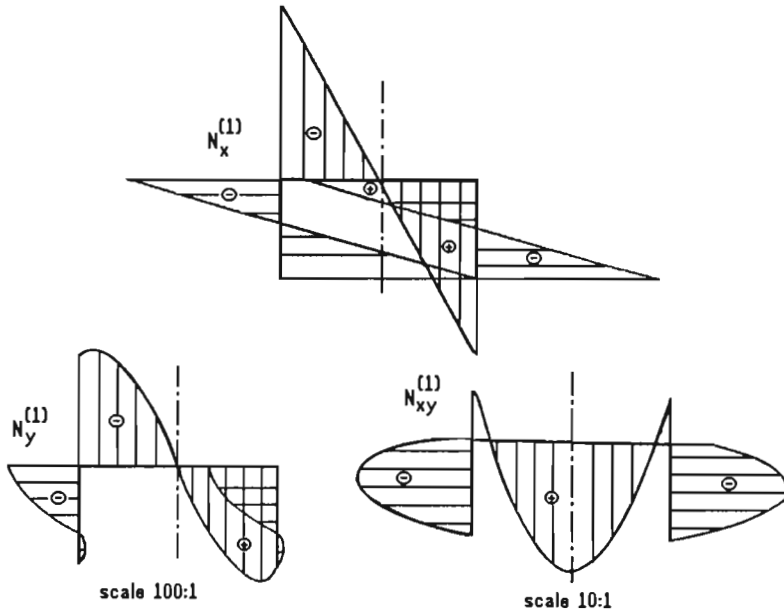


Fig. 10. Plots of in-plane stress resultants  $N_x^{(1)}$ ,  $N_y^{(1)}$ ,  $N_{xy}^{(1)}$  for the flexural-torsional buckling mode

Subsequent Fig.10 and Fig.11 present exemplary plots of in-plane stress resultants  $N_{ix}^{(1)}$ ,  $N_{iy}^{(1)}$ ,  $N_{ixy}^{(1)}$  distributions for the flexural-torsional and the purely flexural one, respectively. The in-plane stress resultants  $N_{ix}^{(1)}$  for both the global modes and  $N_{ixy}^{(1)}$  for the global Euler mode are of the same order and they cannot be neglected since the maximum error is more than 10%.

Fig.12 shows the global modes for an open column, its geometrical dimensions being as follows

$$\begin{array}{llll} \frac{b_1}{b_2} = 0.3077 & \frac{b_3}{b_2} = 0.3077 & \frac{h_1}{h_2} = 0.8 & \frac{h_3}{h_2} = 0.8 \\ \frac{l}{b_2} = 5.0 & \frac{b_2}{h_2} = 52.0 & \nu = 0.3 & \end{array}$$

The primary global buckling mode refers to the Euler's one, while the secondary global mode corresponds to the flexural-torsional one.

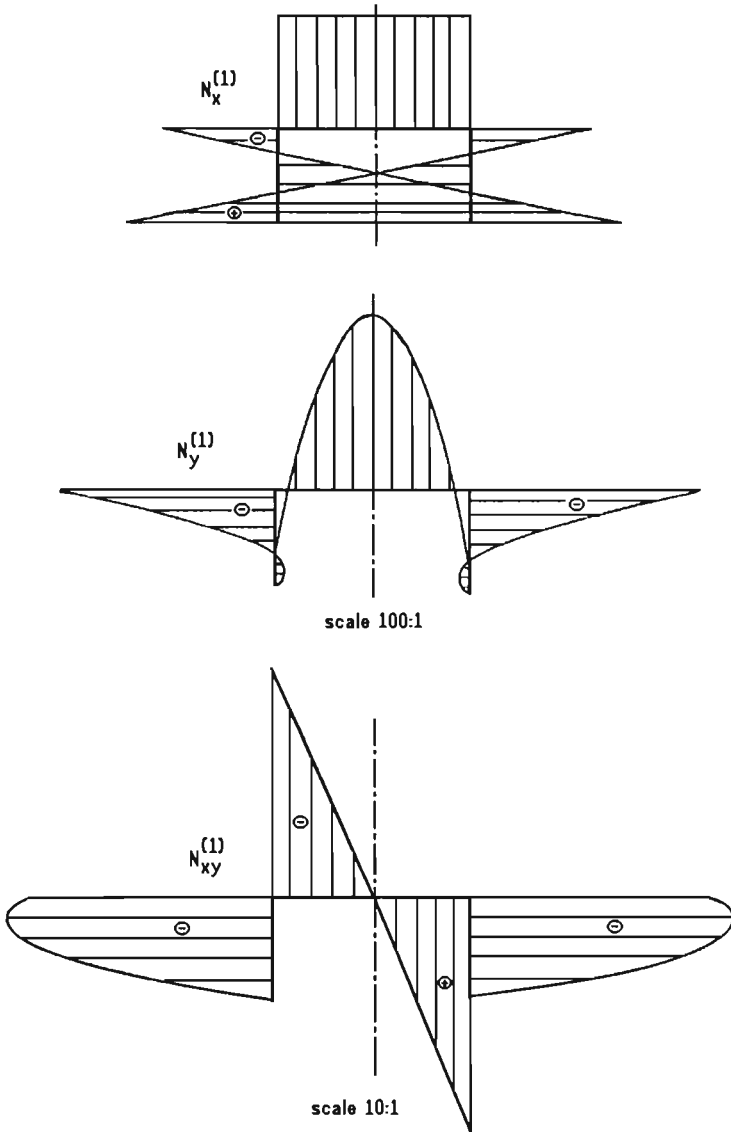


Fig. 11. Plots of in-plane stress resultants  $N_x^{(1)}$ ,  $N_y^{(1)}$ ,  $N_{xy}^{(1)}$  for the purely flexural buckling mode

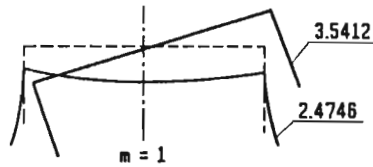


Fig. 12. Global buckling modes for open column

Special attention must be paid to the fact that and in this case the plate model for the global mode should be assumed.

A comparison of results presented in Fig.8a, Fig.9a and Fig.12 clearly shows that an allowance for displacement fields,  $u_i^{(n)}$ ,  $v_i^{(n)}$  and  $w_i^{(n)}$  causes a decrease of the theoretical value of global critical load in relation to the theoretical value of global critical load for a bar-beam model as the slenderness ratio of column becomes lower.

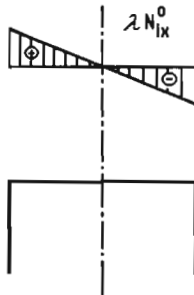


Fig. 13. Cross-section and stress distribution for open beam

The open channel beam loaded by equal and opposite bending moments at the ends, which result in a constant bending moment throughout the beam whose geometrical dimensions are

$$\begin{aligned} \frac{b_1}{b_2} &= 0.5 & \frac{h_1}{h_2} &= 0.5 & \frac{l}{b_2} &= 7.8 \\ \frac{b_2}{h_2} &= 50 & \nu &= 0.3 \end{aligned}$$

Overall buckling therefore takes place as lateral buckling. The lateral global stress value  $\sigma_1^*$  for the plate model is equal to 4.619 and for bar-beam model is determined as equal to 5.484. The lateral buckling mode is illustrated in Fig.14.

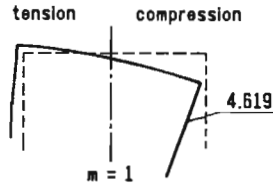


Fig. 14. The lateral buckling mode for open beam

The next figure (Fig.15) presents the exemplary plots of in-plane stress resultants  $N_{ix}^{(1)}$ ,  $N_{iy}^{(1)}$ ,  $N_{ixy}^{(1)}$  for the lateral buckling mode. The resultants  $N_{ix}^{(1)}$ ,  $N_{ixy}^{(1)}$  are the components that can be taken in the buckling analysis. Rational dimensions of the column-beams can be determined on the assumption of the plate model.

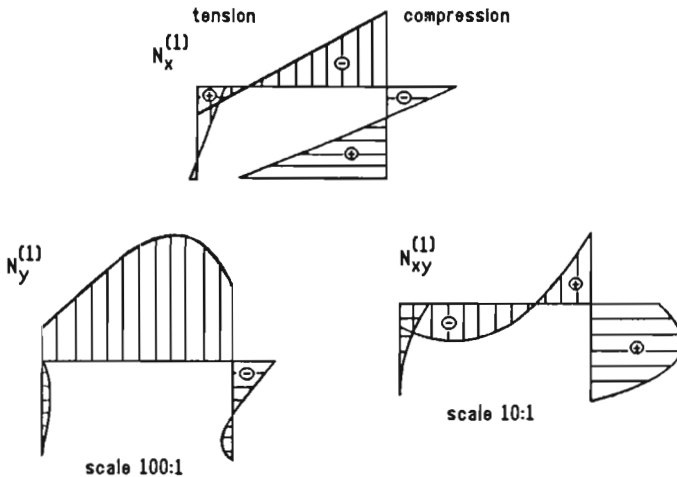


Fig. 15. Plots of in-plane resultants  $N_x^{(1)}$ ,  $N_y^{(1)}$ ,  $N_{xy}^{(1)}$  for the lateral buckling mode

In all cases analysed a plate model was adopted for the description of global buckling. This leads to a lowering of the theoretical value of limiting load, as the characteristic curve for independent mode of buckling is not symmetrical.

For a column-beam with the double symmetrical cross-section regarding only one local buckling mode of a perfect beam (for an uncoupled local buckling) a stable-symmetric post buckling equilibrium was obtained.

For a beam with a single symmetry axis of the cross-section, taking into account only the uncoupled local one, a stable-asymmetric post buckling path



was obtained (for more detailed analysis (cf Kolakowski, 1993)).

Unsignificant changes in the load and geometrical parameters of the structure may in some cases lead to substantial qualitative and quantitative differences (cf Kolakowski, 1989a,b).

#### 4. Conclusions

The buckling analysis of thin-walled closed and open cross-section beams under axial compression and a constant bending moment by means of the transition matrix method has been presented. Global and local modes are described by the von Karman's plate theory.

Attention was paid to the influence of displacements  $u_i^{(n)}$ ,  $v_i^{(n)}$  and  $w_i^{(n)}$  upon critical load values and upon the post-critical behaviour for uncoupled bucklings.

The applied method describing buckling of thin-walled structures from global to local loss of stability can be easily adopted in computer-aided systems, CAD/CAM.

#### References

1. ALI M.A., SRIDHARAN S., 1988, *A versatile model for interactive buckling of columns and beam-columns*, Int.J.Solids Structures, **24**, 5, 481-486
2. BENITO R., SRIDHARAN S., 1984-85, *Mode interaction in thin-walled structural members*, J.Struct.Mech, **12**, 4, 517-542
3. BILSTEIN W., 1974, *Beitrag zur Berechnung vorverformter mit diskreten Längssteifen ausgesteifter, ausschliesslich in Längsrichtung belasteter Rechteckplatten nach der nichtlinearen Beultheorie*, Der Stahlbau, **7**, 193-201 and **9**, 276-282
4. BYSKOV E., HUTCHINSON J.W., 1977, *Mode interaction in axially stiffened cylindrical shells*, AIAA J., **15**, 7, 941-948
5. KLÖPPEL K., BILSTEIN W., 1971, *Ein Verfahren zur Ermittlung der Beulasten beliebiger rechtwinkling abgekanteter offener und geschlossener Profile nach der linearen Beultheorie unter Verwendung eines abgewandelten Reduktionsverfahrens*, Veröffentlichungen des Institutes für Statik und Stahlbau der Technischen Hochschule, Darmstadt, **16**
6. KLÖPPEL K., Schmied R., Schubert J., 1966, *Die Traglast mittig und aussermittig gedrückter dünnwandiger Kastenträger unter Verwendung der nichtlinearen Beultheorie*, Der Stahlbau, **11**, 321-337

7. KOITER W.T., 1976, *General theory of mode interaction in stiffened plate and shell structures*, WTHD Report 590, Delft, 41
8. KOŁAKOWSKI Z., 1987a, *Mode interaction in thin-walled trapezoidal column under uniform compression*, Thin-Walled Structures, 5, 329-342
9. KOŁAKOWSKI Z., 1987b, *Mode interaction in wide plate with closed section longitudinal stiffeners under compression*, Engineering Transactions, 35, 4, 591-609
10. KOŁAKOWSKI Z., 1988, *Some aspects of mode interaction in thin-walled stiffened plate under uniform compression*, Engineering Transactions, 36, 1, 167-179
11. KOŁAKOWSKI Z., 1989a, *Mode interaction in wide plate with angle section longitudinal stiffeners under compression*, Engineering Transactions, 37, 1, 117-135
12. KOŁAKOWSKI Z., 1989b, *Interactive buckling of thin-walled beams with open and closed cross-section*, Engineering Transactions, 37, 2, 375-397
13. KOŁAKOWSKI Z., 1989c, *Some thoughts on mode interaction in thin-walled columns under uniform compression*, Thin-Walled Structures, 7, 23-35
14. KOŁAKOWSKI Z., 1993, *Interactive buckling of thin-walled beams with open and closed cross-sections*, Thin-Walled Structures, 15, 159-183
15. MANEVICH A.I., 1981, *Vzaimodejstvie form poteri ustoičivosti szhatoi podkrepnoj paneli*, Stroitel'naya Mekhanika i Raschet Sooruzhenii, 5, 24-29
16. MANEVICH A.I., 1982, *K teorii svyazannoï poteri ustoičivosti podkrepennykh tonkostennykh konstrukcii*, Prikladnaya Matematika i Mekhanika, 46, 2, 337-345
17. MANEVICH A.I., 1985, *Ustoičivost' oboloček i plastin s rebrami tavrovogo profilya*, Stroitel'naya Mekhanika i Raschet Sooruzhenii, 2, 34-38
18. MANEVICH A.I., 1988, *Svyazannaya poterya ustoičivosti szhatoi podkrepnoj paneli*, Mekhanika Tverdogo Tela, 5, 152-159
19. MOELLMANN H., GOLTERMANN P., 1989, *Interactive buckling in thin-walled beams*, Part I, Theory, Part II, Applications, Int.J.Solids Structures, 25, 7, 715-728, 729-749
20. PIGNATARO M., LUONGO A., 1987, *Asymmetric interactive buckling of thin-walled columns with initial imperfections*, Thin-Walled Structures, 5, 5, 365-386
21. SRIDHARAN S., ALI M.A., 1985, *Interactive buckling in thin-walled beam-columns*, J.of Engng.Mech. ASCE, 111, 12, 1470-1486
22. SRIDHARAN S., ALI M.A., 1986, *An improved interactive buckling analysis of thin-walled columns having doubly symmetric sections*, Int.J.Solids Structures, 22, 4, 429-443
23. SRIDHARAN S., PENG M.H., 1989, *Performance of axially compressed stiffened panels*, Int.J.Solids and Structures, 25, 8, 879-899
24. UNGER B., 1969, *Elastisches Kippen von beliebig gelagerten und aufgehängten Durchlaufträgern mit einfachsymmetrischen, in Trägerachse veränderlichem Querschnitt und einer Abwandlung des Reduktionsverfahrens als Lösungsmethode*, Dissertation D17, Darmstadt

## O pewnych aspektach globalnych i lokalnych postaci wyboczenia w cienkościennych słupach-belkach

### Streszczenie

Projektowanie cienkościennych słupów-belek musi uwzględniać globalne niestateczności oraz niestateczności płyt składowych odpowiadających wyboczeniu lokalnemu. Praca poświęcona jest cienkościennym sprężystym belkom o zamkniętych i otwartych przekrojach poprzecznych poddanych ścisaniu osiowemu i zginaniu. Na końcach założono swobodne podparcie. Zastosowano asymptotyczne rozwinięcie Byškova i Hutchinsona przy wykorzystaniu numerycznej metody macierzy przeniesienia. Obliczenia przedstawiono dla różnych typów belek.

*Manuscript received April 7, 1993; accepted for print August 18, 1993*